

# Stir casting process for manufacture of Al–SiC composites

Shahin Soltani, Rasoul Azari Khosroshahi,  
Reza Taherzadeh Mousavian\* ,  
Zheng-Yi Jiang, Alireza Fadavi  
Boostani, Dermot Brabazon

S. Soltani, R. Azari Khosroshahi, R. Taherzadeh Mousavian\* Faculty of Materials Engineering, Sahand University of Technology, Tabriz 37200-000, Iran  
e-mail: rtaher1898@gmail.com; r\_taherzadeh@sut.ac.ir

Z.-Y. Jiang, A. Fadavi Boostani  
School of Mechanical, Materials and Mechatronic Engineering, University of Wollongong, Wollongong, NSW 2522, Australia

D. Brabazon  
Advanced Processing Technology Research Centre, School of Mechanical and Manufacturing Engineering, Dublin City University, Dublin 9, Ireland

## Abstract

Stir casting is an economical process for the fabrication of aluminum matrix composites. There are many parameters in this process, which affect the final microstructure and mechanical properties of the composites. In this study, micron-sized SiC particles were used as reinforcement to fabricate Al-3 wt% SiC composites at two casting temperatures (680 and 850 °C) and stirring periods (2 and 6 min). Factors of reaction at matrix/ceramic interface, porosity, ceramic incorporation, and agglomeration of the particles were evaluated by scanning electron microscope (SEM) and high-resolution transition electron microscope (HRTEM) studies. From microstructural characterizations, it is concluded that the shorter stirring period is required for ceramic incorporation to achieve metal/ceramic bonding at the interface. The higher stirring temperature (850 °C) also leads to improved ceramic incorporation. In some cases, shrinkage porosity and intensive formation of  $Al_4C_3$  at the metal/ceramic interface are also observed. Finally, the mechanical properties of the composites were evaluated, and their relation with the corresponding microstructure and processing parameters of the composites was discussed.

## Keywords

Aluminum matrix composite; Microstructure; Mechanical properties; Stir casting

## 1 Introduction

Aluminum metal matrix composites (AMMCs) have gained significant attention in recent years. This is primarily due to their lightweight, low coefficient of thermal expansion (CTE), good machinability, and improved mechanical properties, such as 0.2 % yield stress (YS), ultimate tensile stress (UTS), and hardness. Owing to these advantages, they are used in aerospace (e.g., airframe components), automobile (e.g., engine pistons), and electronic (e.g., integrated circuit mounting frame components) industries [1–8].

Stir casting (vortex technique) is generally accepted commercially as a low-cost method for fabrication of AMMCs. Its advantages lie in its simplicity, flexibility, and applicability to large volume production. This process is the most economical among all the available routes for AMMCs production, and it allows very large-sized components to be fabricated. However, the following considerations for achieving AMMC via stir casting must be considered: no adverse chemical reaction between the reinforcement material and matrix alloy, no or very low porosity content in the cast AMMCs, wettability between the two main phases, and a uniform distribution of the reinforcement material. Wettability and reactivity determine the quality of the bonding between the constituents and thereby greatly affect the final properties of the composite material [9–16].

The addition of alloying elements can modify the matrix metal alloy by producing a transient layer between the particles and the liquid matrix. This transient layer has a low wetting angle, decreases the surface tension of the liquid, and surrounds the particles with a structure that is similar to both the particle and the matrix alloy [3, 9, 11, 12]. Our previous study [3] indicated that Mg was the best metal among Ca, Ti, Zn, Si, and Zr for increasing the incorporation fraction of micron-sized SiC particles by molten pure aluminum.

In this study, micron-sized SiC particles were used as reinforcement of pure aluminum to fabricate as-cast aluminum matrix composite, and Mg (1 wt%) was added to improve the wettability and incorporation fraction of ceramic particles. The main aim of this study is to lessen the number of defect locations within AMMCs produced from the stir casting method and hence to improve the quality of the fabricated composites. Therefore, reaction at matrix/ceramic interface, porosity, ceramic incorporation, and agglomeration of particles were evaluated. The mechanical properties of the composites were also investigated, and their relation with the corresponding microstructures and processing parameters was discussed.

## 2 Experimental

Aluminum ingot with 99.8 wt% commercial purity was used as a matrix. The chemical composition of the used ingot obtained using a M5000 optical emission spectrometer is given in Table 1.

Micron-sized SiC particles with an average particle size of 80  $\mu\text{m}$  and 99.9 % purity were supplied (Shanghai Dinghan Chemical Co., Ltd. China) as the reinforcement of metal matrix composite. The morphology of the silicon carbide particles used in this study is shown in Fig. 1.

In order to fabricate the composites, 1 g reinforcement SiC powder was encapsulated carefully in an aluminum foil packet for insertion into the molten aluminum in order to fabricate a composite with 3 wt% SiC as reinforcement. These powders were preheated at 350 C for 4 h before the casting process to remove the moisture and impurities. The pure aluminum was heated to various temperatures of 680 and 850 C within a bottom-pouring furnace. A preheated graphite stirrer was placed below the surface of melt and rotated at a speed of 500  $\text{r min}^{-1}$ , and simultaneously argon gas of high purity was used as a protective shroud on the melt surface. Figure 2 shows the schematic of the vortex casting setup used for the stir casting process. The composite slurry was poured into a low-carbon steel mold. 1 wt% Mg was added to the melt to increase the wettability between the matrix and the reinforcements.

Mg acts like a surfactant power, which reduces the aluminum oxide coating by binding to the oxygen. The magnesium reactions with alumina to form  $\text{MgAl}_2\text{O}_4$  spinel at the interface Al/SiC are noted as follows [17–20]:

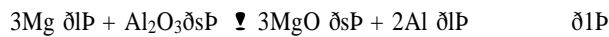


**Table 1** Chemical compositions of used pure aluminum (wt%)

| Al   | Si  | Fe   | Cu   | Mn   | Zn   | Ni   | Pb    | Sn    |
|------|-----|------|------|------|------|------|-------|-------|
| 99.8 | 0.1 | 0.04 | 0.01 | 0.01 | 0.02 | 0.01 | 0.005 | 0.004 |

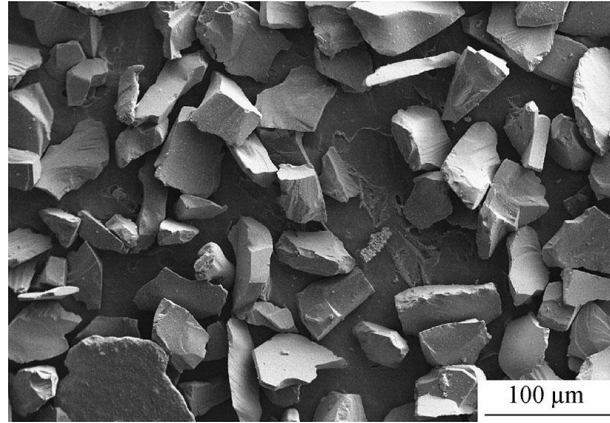


Fig. 1 SEM image of SiC particles used as reinforcement

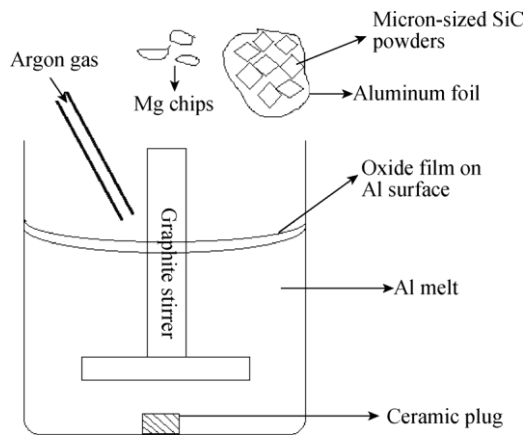


Fig. 2 Schematic of stir casting set-up used for fabrication of composites

The process parameters of the three fabricated samples in this study are shown in Table 2. Generally, a lower stirring time is beneficial for three important reasons. Firstly, a lower casting duration is economically preferred; secondly, the reaction between matrix and reinforcement occurs over a period of time, meaning that this detrimental phenomenon could be avoided using a lower stirring period; and thirdly, a higher casting duration might lead to entrapment of a larger amount of porosity after solidification [21]. Therefore, Sample 1 was investigated in this study to examine whether further stirring after particle feeding was necessary or not. The ceramic particles for Sample 1 were given no additional period after this particle feeding process to aid incorporation and distribution within the molten metal. As shown in Table 2, the process of particle feeding during casting lasted for 2 min for all the samples. For Samples 2 and 3, the stirring was continued for an extra 4 min after the 2-min particle feeding process.

The specimens were prepared for metallographic examinations using 220–320–500–1000 mesh emery papers, followed by polishing with 1- $\mu\text{m}$  sized diamond paste. Microscopic methods were used to study the composite structure and fracture surface by two kinds of scanning electron microscopes (SEM, Cam Scan Mv2300, equipped with energy-dispersive X-ray spectroscopy (EDX) analysis and SEM, KYKY-EM3200), and an optical microscope (OM). A high-resolution transmission electron microscope (HRTEM, Philips CM200) at an accelerating voltage of 200 kV was also used to study the reaction at the interface of the aluminum matrix and SiC particles.

Microhardness tests were conducted according to ASTM E384 using an applied load of 0.49 N for a 15 s. At least ten measurements were taken from fabricated samples. Tensile specimens were also prepared from the as-cast composites. All of the tensile tests were performed at room temperature using an Instron testing machine operating at a constant rate of crosshead displacement, with an initial strain rate of  $2.9 \times 10^{-3} \text{ s}^{-1}$ .

The 0.2 % proof strength (interpreted as the measurable yield strength, YS), ultimate tensile strength (UTS), and ductility (% elongation to break) were measured and averaged over three test samples. The density of the samples was measured also using Archimedes' principle. Distilled water was used as the immersion fluid. Theoretical density was calculated and compared with the measured densities. The amount of ceramic particles incorporated into the molten aluminum was determined by leaching the composite using 2 mol L<sup>-1</sup> hydrochloric acid, resulting in the removal of aluminum phase. The undissolved residue was then separated from the solution by filtration.

In order to determine the onset reaction temperature between pure aluminum and SiC powders, differential scanning calorimetry (DSC, Netzsch STA 409, Germany) was performed. For this purpose, the same weight of aluminum and SiC powders were mixed for 30 min using a low-energy ball mill to make a suitable contact between them and break any possible oxide layer on the aluminum surface. The milled powders were then heated from 25 to 800 °C at a heating rate of 10 °C min<sup>-1</sup> using pure argon atmosphere and alumina crucible.

### 3 Results and discussion

#### 3.1 SEM and OM studies of composite microstructures

Figures 3, 4, and 5 show SEM images of the fabricated Samples 1–3, respectively. Figure 3a shows the microstructure of Sample 1, in which just after ceramic feeding for 2 min, the stirring process is stopped. And the amount of ceramic particles incorporated seems to be insignificant for Sample 1, showing that further stirring is necessary for the powders to be well incorporated into the melt. The visual examinations indicate that a large fraction of powders remain on the surface of the melt and adhere to the crucible wall. The presence of gas pores is also evident in this microstructure. It was reported that the porosity in cast MMCs was originated from gas entrapment during stirring, water vapor (H<sub>2</sub>O) on the surface of ceramic particles, hydrogen evolution, air bubbles entering the slurry as an air envelope to the reinforcement particles, and shrinkage during solidification process [9].

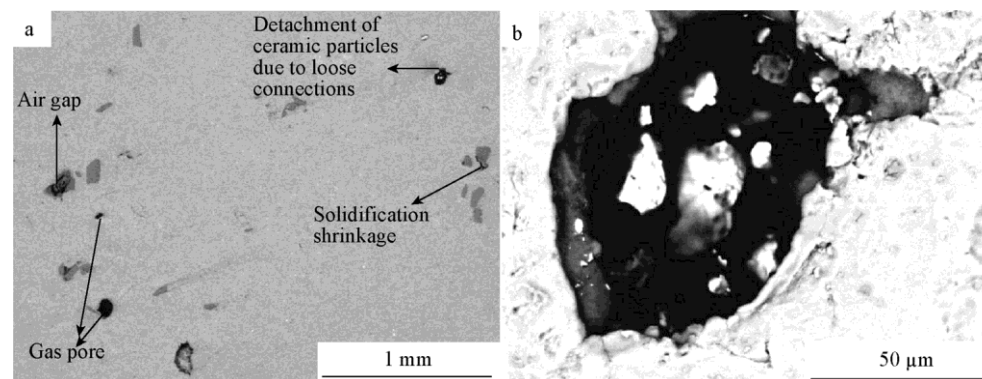


Fig. 3 SEM images of Sample 1 after stir casting with different magnifications

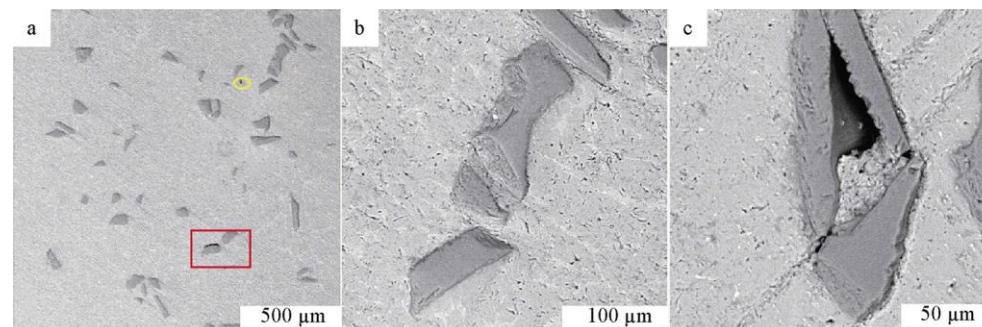


Fig. 4 SEM images of Sample 2 after stir casting with different magnifications

Owing to preheating of the SiC powders at 350 C, no water vapor would be present on the ceramic surfaces. It seems that gas entrapment occurs especially at the lower temperature of 680 C; in comparison with the 850 C processing temperature, and the viscosity of the melt is higher at 680 C. This may affect generated gas escape and thereby increase the porosity level. Solidification shrinkage is found in just one location (Fig. 3a), and the reason of defect is not highly evident at this temperature, while an air gap between the agglomerated particles is observed in Fig. 3a. Figure 3b shows the phenomenon of particle detached from the matrix after the polishing process to prepare the samples for microstructural characterization. It indicates that the particle distribution is not adequate in this sample. Owing to a direct contact between molten aluminum and SiC particles,  $Al_4C_3$  could be formed at the interface [22– 25]. It was reported that a layer of aluminum carbide ( $Al_4C_3$ ) was found to increase YS, UTS, and work hardening rate, and change the fracture pattern from one involving interfacial decohesion to one where particle breakage was dominant [23]. Although the stirring temperature is 680 C for Sample 1, it seems that no bonding reaction occurs for this sample.

Figure 4a shows the microstructure of Sample 2 cast at 680 C with stirring for 4 min and post-particle addition. The presence of gas pore and solidification shrinkage is highlighted by the yellow-colored circle and red-colored rectangles, respectively. It is important to note that a lower amount of gas pores could be seen in this sample, indicating that the further stirring and fluid flow in the slurry aid the entrapped gas to escape from the melt, even though this extra period might attract further gas into the melt from the environment. As it can be seen, the amount of ceramic entrapped particles is considerable for this sample, showing that mechanical stirring is a real factor for improved ceramic particle incorporation by molten metal. An important result from Fig. 4b is that AMMC can be formed with a relative defect-free interface between matrix and reinforcement. The ceramic particles seems to be well adhered to the matrix, and no detachment of particles from the matrix could be seen during sample preparation for microstructural study. The additional stirring period is therefore a very important parameter for achieving desired interfacial reactions. Figure 4c shows that the entrance of air among clustered particles could also be seen in Sample

2. In fact, it seems that the use of mechanical stirring method under these conditions could not avoid the formation of agglomerated particles at 680 C, and the porosity in this sample might emanate from the air gap between the ceramic particles.

Figure 5a shows the microstructure of Sample 3 cast at 850 C, in which the ceramic particles were stirred for 6 min. As it can be seen, considerable amounts of ceramic particles are incorporated into the matrix at this temperature. It was reported that SiC particles had a higher wettability by molten aluminum at higher temperatures [12]. Figure 5a confirms that Sample 3 contains the highest amount of ceramic particles. Another important matter is the presence of round-shaped gas pores, which have the average diameter of less than 10  $\mu m$ . An intensive attraction of environmental gas occurs for Sample 3 at 850 C for aluminum alloys [26–29]. Like other two samples, agglomeration of ceramic particles could be observed for Sample 3. However, the distribution of ceramic particles seems to be better for Sample 3 than for Samples 1 and 2. Figure 5a shows some particles that are well bonded to the matrix. However, Fig. 5b shows the considerable occurrences of particle detached from the matrix. From the reaction occurrence view, it might be concluded that this should be due to the intensive formation of brittle  $Al_4C_3$  compound with a higher thickness that causes a reduction in the interface strength, while Fig. 5c indicates that intensive shrinkage porosity occurs for Sample 3 during solidification and this shrinkage enables the detachment of particles from the matrix. As it can be seen from Fig. 5c, even a crack in the matrix is formed as a result of the sudden reduction of temperature from 850 C to room temperature (no preheating was applied for the mold). Figure 5c also demonstrates that an air gap between the particles also occurs for Sample 3 production settings.

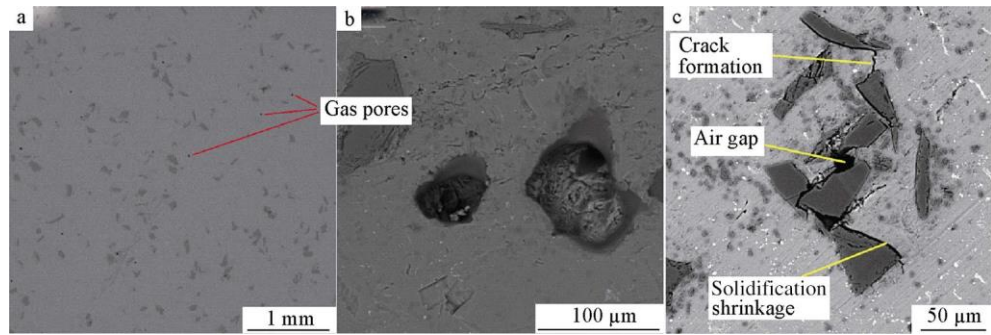


Fig. 5 SEM images of Sample 3 after stir casting with different magnifications

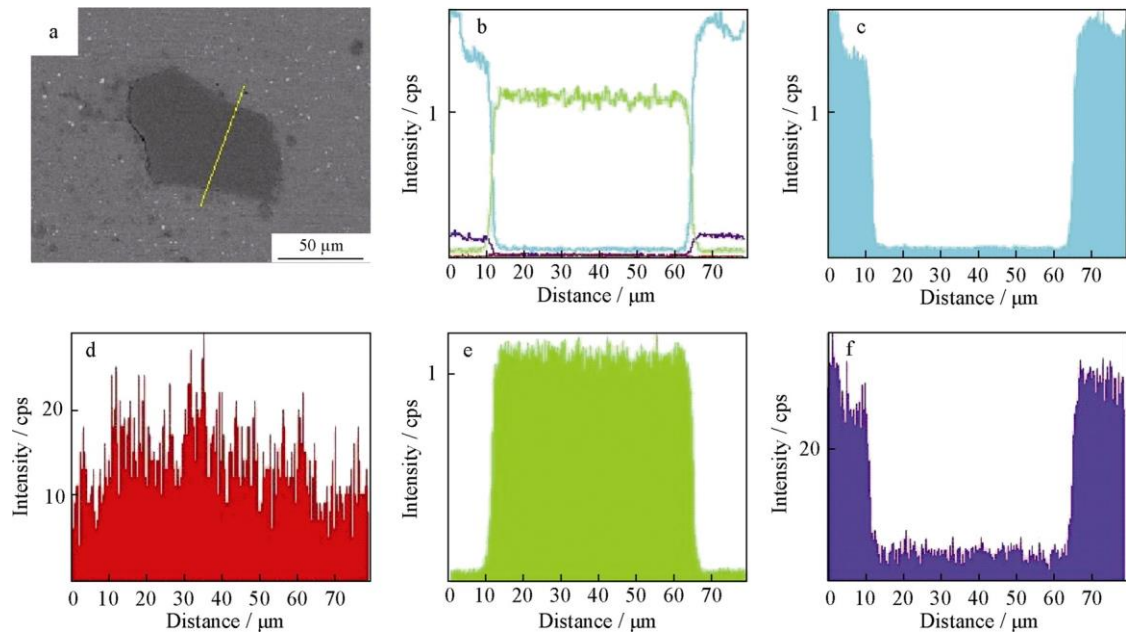


Fig. 6 SEM image a, corresponding line scanning map b, and EDX elemental analysis around a ceramic particle in Sample 3: c Al, d C, e Si, and f Mg

Line energy dispersive X-ray spectroscopy (EDX) microanalysis (Fig. 6) was used to evaluate the chemical characterization around a ceramic particle in Sample 3.

As shown in Fig. 6, Mg is present at the Al/SiC interface and in the matrix of aluminum with the same intensity, indicating the good Al–Mg alloy fabrication.

OM analysis was used in this study to compare the grain size of the matrix alloy after composite solidification of Samples 2 and 3 (Fig. 7a, b). Solidification from the higher temperature of 850 C results in a lower grain size in Sample 3 (Fig. 7b) compared with that from the lower processing temperature of 680 C in Sample 2 (Fig. 7a). The lower processing temperature would be expected to lead to a lower cooling rate and hence larger grain size. This would affect the mechanical properties based on Hall–Petch equation [30].

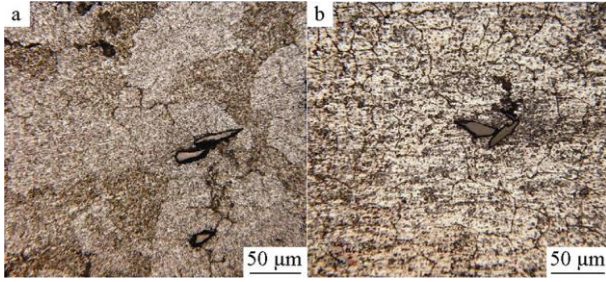


Fig. 7 OM images of as-cast Sample 2 a and Sample 3 b

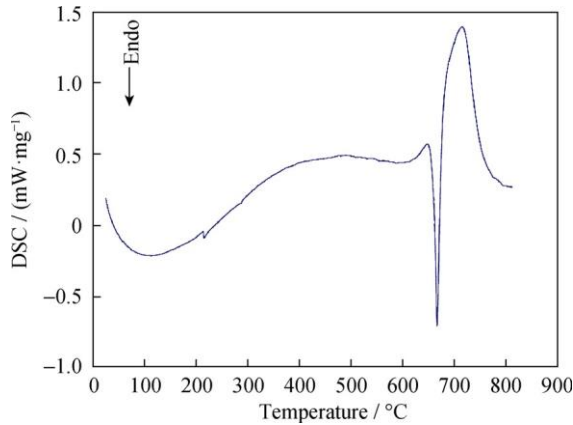


Fig. 8 DSC analysis of Al-SiC powder mixture

### 3.2 Reaction between aluminum matrix and SiC particles

It was reported previously that at temperatures of 657– 827 C, SiC interacted with aluminum via a dissolution– precipitation process [24, 31]. This mechanism involves the migration of carbon atoms from places where the SiC surface is in direct contact with the aluminum to the growing faces of  $\text{Al}_4\text{C}_3$  crystals located at or close to the aluminum/SiC interface. The  $\text{Al}_4\text{C}_3$  brittle compound has detrimental influences on the composite and reduces its strength and ductility. It also reacts with liquid water or moisture in the ambient atmosphere, deteriorating the properties further [32].  $\text{Al}_4\text{C}_3$  would be formed based on Eq. (3) [33]:



The reaction is thermodynamically possible because that the standard free energy change for this reaction is negative, and  $\text{Al}_4\text{C}_3$  and Si are the two major interfacial reaction products [25, 31, 33]. As mentioned, the migration of carbon atoms (exchange of atoms) is involved in a chemical reaction, leading to wettability and bonding improvement. Therefore, it seems that  $\text{Al}_4\text{C}_3$  formation to a small extent may be required for the bonding between SiC and aluminum [34]. However, increased reaction between Al and SiC due to a long exposure time or a very high casting temperature can lead to the formation of a thicker layer of  $\text{Al}_4\text{C}_3$  which might make the AMMC brittle [34].

Figure 8 shows the thermal analysis of the ball-milled Al-SiC mixture. As can be seen, the on-set of aluminum melting is evident from about 650 C (endothermic peak) and just after this, an exothermic trend could be observed, which corresponds to the occurrence of a reaction between Al and SiC, leading to a large release of heat. Figure 8 shows that Al and SiC mainly react with each other just after the melting of aluminum.

In order to evaluate the reaction occurrence between Al and SiC and observe the bonding of SiC with aluminum matrix, HRTEM analysis was used for all the samples. Figure 9a shows the nanostructure of Sample 1. As can be seen, a relatively clean interface is formed between crystalline SiC and aluminum matrix, and no trace of  $\text{Al}_4\text{C}_3$  can be observed at or near the interface. Stirring for 2 min at 680 C is not a

long-enough period or high-enough temperature combination process for the migration of carbon atoms and the formation of suitable bond between Al and SiC particles. It was reported that  $\text{Al}_4\text{C}_3$  appeared as needle-like slice-like features on the interface toward the matrix side in HRTEM images [35]. Figure 9b shows the nanostructure of Sample 2, in which particles are exposed to the molten aluminum with stirring for 6 min. A very good physical bonding seems to be formed for Sample 2 between the Al and crystalline SiC. After characterization, needle-like  $\text{Al}_4\text{C}_3$  phase is detected with a different orientation growth from the crystalline plane orientations of silicon carbide. However, it should be noted that the size of this needle-like phase seems to be less than 8 nm in height. It is interesting to note that from this finding this phase could be fabricated after stirring for 6 min at 680 C. For Sample 3 produced at 850 C, it is found that the exposure of SiC with molten aluminum at 850 C highly affects the formation and growth of  $\text{Al}_4\text{C}_3$  phase even after stirring for only 6 min. Figure 9c shows the nanostructure of Sample 3. As it can be seen,  $\text{Al}_4\text{C}_3$  with a height of about 120 nm is easily detected at the Al/SiC interface. The selected area diffraction (SAD) pattern of the corresponding phase confirms its formation with a crystalline structure.

From the SEM and TEM results presented above, a summary of the effects of the processing parameter settings on interface compound formation, ceramic incorporation fraction, and ceramic agglomeration is presented in Table 3. It can be seen that only 32 % incorporation occurs for Sample 1, while for Samples 2 and 3, respectively, about 88 % and 97 % particles enter into the molten pure aluminum, meaning that stirring time and temperature highly affect the ceramic incorporation. Kobashi and Choh [36] reported that there is an incubation time for the ceramic particles to incorporate into the molten aluminum, meaning that it is not reasonable to stop the stirring process just after particle feeding, and also it can be concluded that no required interface would be obtained between the ceramics and matrix for a short stirring time. It was also reported that by increasing the stirring temperature, the wettability of the ceramic particles might be improved, resulting in a higher value of ceramic incorporation fraction [12].

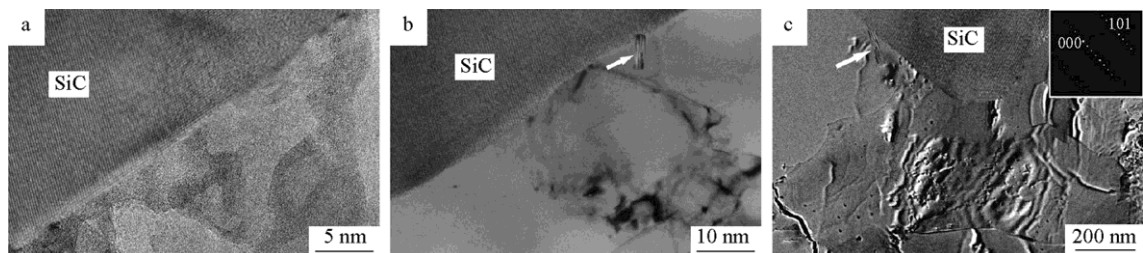


Fig. 9 HRTEM images of as-cast samples: a Sample 1, b Sample 2, and c Sample 3

### 3.3 Mechanical properties and fractograph analysis

Tensile and Vickers microhardness tests were conducted in order to evaluate the effects of these processing conditions and resultant structures on the mechanical properties. Table 4 shows the results of relative densities of the samples.

As it can be seen from Table 4, there is no significant difference in relative density among the samples. As mentioned, the type of porosity and its shape highly affect the mechanical properties. Round-shaped pores do not reduce the tensile strength and ductility as much as jaggedlike shrinkage pores due to the lower stress concentration of the round pore shape. The jagged shrinkage pores can be expected to lower bonding strength at the matrix/ceramic interface, which is associated with macroscale mechanical properties of the composite. Another is the thermal expansion coefficient difference between SiC and Al. The thermal expansion coefficient of SiC is about  $4.9 \times 10^{-6} \text{ C}^{-1}$  and that of Al alloy is greater than  $20.9 \times 10^{-6} \text{ C}^{-1}$ . Entrapment of the particles can also induce physical strains. The associated internal stress will arise in the composite materials, leading to the formation of dislocations around the particles, which could strengthen the composite [37–40]. It should be noted that if the cooling rate is too fast, then

the resulting internal stress might be too large. If these stresses exceed the maximum strength of the aluminum alloy, this phase might crack in addition to the more brittle SiC phase [37, 41, 42].

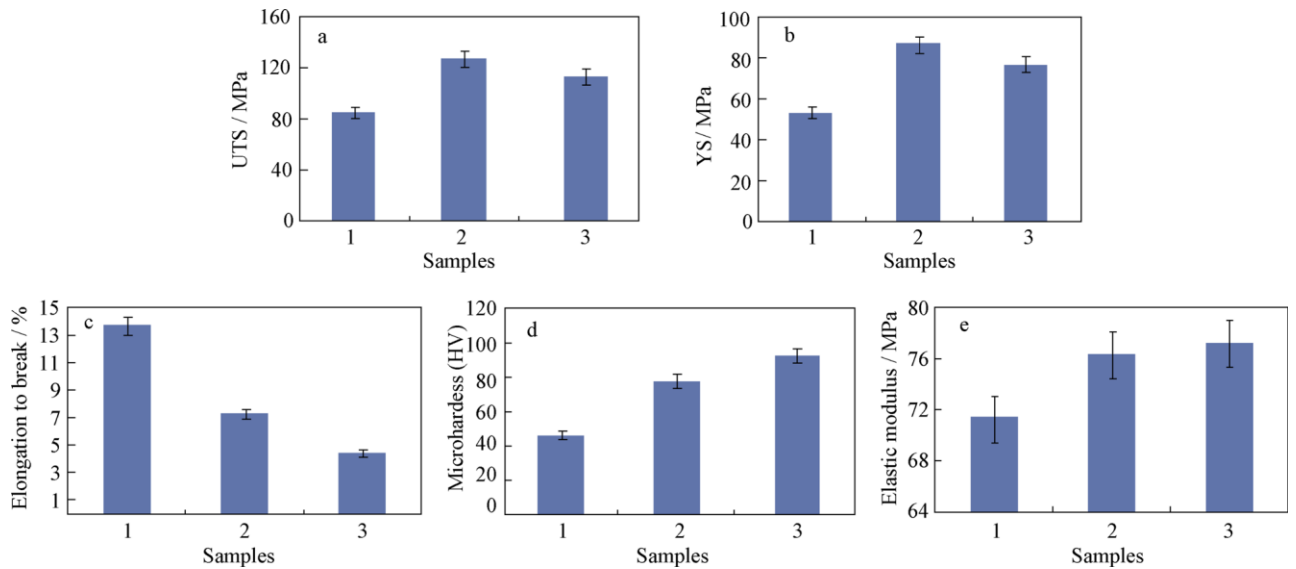


Fig. 10 Mechanical properties of as-cast samples: a UTS, b YS, c elongation to break, d microhardness, and e elastic modulus

Figure 10 shows the results of tensile and microhardness tests. As it can be seen, the values of average microhardness increase by increasing the amount of ceramic particles. Figures 3, 4, and 5 indicate that Sample 3 has the highest amount of ceramic particles, followed by Samples 2 and 1 in turn. As can be observed, the YS and UTS values of Sample 2 are higher than those of Sample 1 due to the presence of a larger amount of ceramic particles. However, this trend could not be seen for Sample 3, in which lower YS and UTS values are obtained in comparison to Sample

2. The considerable formation of shrinkage porosity at the interface significantly reduces the strength of the composite, even though it has a larger amount of ceramic particle incorporations. However, it is not clear that the formation of  $Al_4C_3$  (Fig. 9c) could adversely affect the bonding and strength of the composite. Sample 3 has a smaller grain size with respect to Sample 2 (Fig. 7). However, this slight difference in grain size would not be sufficient to make Sample 1 significantly stronger than Sample 2. Figure 10 also shows the values of ductility for these samples. A higher ductility is obtained for Sample 1 that contains the lowest amount of entrained ceramic particles. In fact, the presence of ceramic particles, especially in micrometer range, causes a considerable reduction in ductility of Samples 2 and 3 compared to that of Sample 1. A higher reduction in ductility of Sample 3 might be due to the poor interface quality. Therefore, it could be concluded that the presence of ceramic particles and the formation of shrinkage porosities around the particles are the two most important factors in determining the AMMC ductility as well as the mechanical properties in general. Figure 10e is the results of elastic modulus of the samples. It can be seen that there is an increasing trend with the increase in the content of ceramic particles of Samples 1–3.

The relationship between the AMMCs strength and particle/matrix interfacial bonding strength is the critical criterion to determine the fracture mode of the composites. If the particle/matrix interfacial bonding strength is high, particle fracture usually happens during deformation. On the other hand, if the particle/matrix interfacial bonding strength is weak, decohesion between the SiC particles and the aluminum matrix will occur prior to the particle fracture [40–43]. Figure 11a shows a particle fracture mode for Sample 2 with strong bonding. The presence of dimples in the matrix is also evident for this sample. It appears that the matrix deformation occurs first followed by ceramic particle fracture. The micrograph in Fig. 11b clearly shows that particle debonding takes place at particle–matrix interface. The cracks around the SiC particles are also evident for Sample 2. Figure 11b shows that debonding of SiC particles takes place before the deformation of matrix. No facet could be seen on the matrix fracture surface, indicating that the matrix fails in ductile mode as expected.

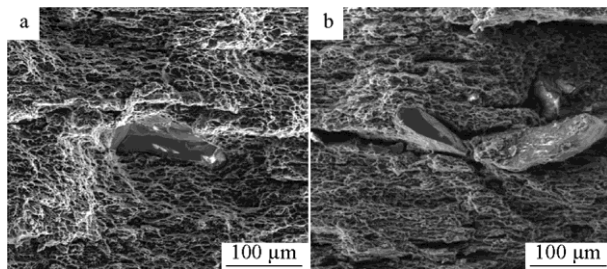


Fig. 11 SEM images of fracture surfaces of Sample 2 a and Sample 3 b

#### 4 Conclusion

Micron-sized SiC particles were incorporated into a melt of pure aluminum with the aid of Mg addition as a wetting agent to fabricate aluminum matrix composite. Two casting temperatures and stirring time were applied to focus on the ceramic particle incorporation, porosity formation, agglomeration of ceramic particles, and interfacial reactions between Al and SiC.

No suitable bonding was obtained at the metal/ceramic interface for the stirring time of 2 min, indicating that a minimum stirring time is necessary for ceramic particles to be in contact with the melt to form a strong bond with the matrix. A higher stirring temperature would lead to a further incorporation of ceramic particles into the molten pure aluminum with an improved distribution. However, the reduced mechanical properties from the AMMC formed at 850 C could be attributed to the formation of shrinkage porosity and an increased formation of  $Al_4C_3$  at the Al–SiC interface. Agglomeration of the micron-sized SiC particles could be observed in all the samples, indicating that the stirring time, temperature, and viscosity of the melt could not affect this phenomenon. Gas pores, solidification shrinkage, and air gap between the agglomerated ceramic particles were observed in the samples after stir casting, while by changing the stirring time and temperature, the type and the amount of porosities could be altered. Detachment of ceramic particles from the matrix was observed in some areas when the ceramic particles were not stirred for a suitable time, and the composite was cooled at a high solidification rate. It is found that the sample with a higher amount of ceramic particles is harder than the other samples.

#### References

- [1] Roshan M, Mousavian RT, Ebrahimkhani H, Mosleh A. Fabrication of Al-based composites reinforced with  $Al_2O_3$ – $TiB_2$  ceramic composite particulates using vortex-casting method. *J Min Metall Sect B*. 2013;49(3):299.
- [2] Valibeygloo N, Khosroshahi RA, Mousavian RT. Microstructural and mechanical properties of Al-4.5 wt% Cu reinforced with alumina nanoparticles by stir casting method. *Int J Miner Metall Mater*. 2013;20(10):978.
- [3] Mohammadpour M, Khosroshahi RA, Mousavian RT, Brabazon D. Effect of interfacial-active elements addition on the incorporation of micron-sized SiC particles in molten pure aluminum. *Ceram Int*. 2014;40(6):8323.
- [4] Mohammadpour M, Khosroshahi RA, Mousavian RT, Brabazon D. A novel method for incorporation of micron-sized SiC particles into molten pure aluminum utilizing a Co coating. *Metall Mater Trans B*. 2015;46(1):12.
- [5] Naher S, Brabazon D, Looney L. Development and assessment of a new quick quench stir caster design for the production of metal matrix composites. *J Mater Process Technol*. 2005; 166(3):430.
- [6] Naher S, Brabazon D, Looney L. Computational and experimental analysis of particulate distribution during Al–SiC MMC fabrication. *Compos Part A Appl Sci Manuf*. 2007;38(3):719.
- [7] Mousavian RT, Damadi SR, Khosroshahi RA, Brabazon D, Mohammadpour M. A comparison study of applying metallic coating on SiC particles for manufacturing of cast aluminum matrix composites. *Int J Adv Manuf Technol*. 2015;. doi:10. 1007/s00170-015-7246-4.
- [8] Boostani AF, Tahamtan S, Jiang ZY, Wei D, Yazdani S, Khosroshahi RA, Mousavian RT, Xu J, Zhang X, Gong D. Enhanced tensile properties of aluminium matrix composites reinforced with graphene encapsulated SiC nanoparticles. *Compos A*. 2015;68(2):155.
- [9] Hashim J, Looney L, Hashmi M. Metal matrix composites: production by the stir casting method. *J Mater Process Technol*.

- 1999;92–93:1.
- [10] Naher S, Brabazon D, Looney L. Simulation of the stir casting process. *J Mater Process Technol.* 2003;143:567.
- [11] Hashim J, Looney L, Hashmi M. The enhancement of wettability of SiC particles in cast aluminum matrix composites. *J Mater Process Technol.* 2001;119(1):329.
- [12] Hashim J, Looney L, Hashmi M. The wettability of SiC particles by molten aluminum alloy. *J Mater Process Technol.* 2001; 119(1):324.
- [13] Rajan T, Pillai R, Pai B, Satyanarayana K, Rohatgi P. Fabrication and characterisation of Al–7Si–0.35 Mg/fly ash metal matrix composites processed by different stir casting routes. *Compos Sci Technol.* 2007;67(15):3369.
- [14] Surappa M. Synthesis of fly ash particle reinforced A356 Al composites and their characterization. *Mater Sci Eng A.* 2008;480(1):117.
- [15] Ibrahim I, Mohamed F, Lavernia E. Particulate reinforced metal matrix composites—a review. *J Mater Sci.* 1991;26(5):1137.
- [16] Srivatsan T, Ibrahim I, Mohamed F, Lavernia E. Processing techniques for particulate-reinforced metal aluminum matrix composites. *J Mater Sci.* 1991;26(22):5965.
- [17] Rajan T, Pillai R, Pai B. Reinforcement coatings and interfaces in aluminum metal matrix composites. *J Mater Sci.* 1998; 33(14):3491.
- [18] Schultz B, Ferguson J, Rohatgi P. Microstructure and hardness of Al<sub>2</sub>O<sub>3</sub> nanoparticle reinforced Al–Mg composites fabricated by reactive wetting and stir mixing. *Mater Sci Eng A.* 2011; 530:87.
- [19] Sukumaran K, Pillai S, Pillai R, Kelukutty V, Pai B, Satyanarayana K, Ravikumar KK. The effects of magnesium additions on the structure and properties of Al-7Si-10SiCp composites. *J Mater Sci.* 1995;30(6):1469.
- [20] Candan E, Atkinson HV, Turen Y, Salaoru I, Candan S. Wettability of aluminum–magnesium alloys on silicon carbide substrates. *J Am Ceram Soc.* 2011;94(3):867.
- [21] Prabu SB, Karunamoorthy L, Kathiresan S, Mohan B. Influence of stirring speed and stirring time on distribution of particles in cast metal matrix composite. *J Mater Process Technol.* 2006; 171(2):268.
- [22] Urena A, Martinez E, Rodrigo P, Gil L. Oxidation treatments for SiC particles used as reinforcement in aluminum matrix composites. *Compos Sci Technol.* 2004;64(12):1843.
- [23] Tham L, Gupta M, Cheng L. Effect of limited matrix-reinforcement interfacial reaction on enhancing the mechanical properties of aluminum–silicon carbide composites. *Acta Mater.* 2001;49(16):3243.
- [24] Yan M, Fan Z. Review durability of materials in molten aluminum alloys. *J Mater Sci.* 2001;36(2):285.
- [25] Ureña A, Escalera M, Gil L. Oxidation barriers on SiC particles for use in aluminum matrix composites manufactured by casting route: mechanisms of interfacial protection. *J Mater Sci.* 2002;37(21):4633.
- [26] Monroe R. Porosity in castings. *AFS Trans.* 2005;113:519.
- [27] Lapham D, Schwandt C, Hills M, Kumar R, Fray D. The detection of hydrogen in molten aluminum. *Ionics.* 2002; 8(5–6):391.
- [28] Yi J, Gao Y, Lee P, Flower H, Lindley T. Scatter in fatigue life due to effects of porosity in cast A356-T6 aluminum-silicon alloys. *Metall Mater Trans A.* 2003;34(9):1879.
- [29] Wang Q, Crepeau P, Davidson C, Griffiths J. Oxide films, pores and the fatigue lives of cast aluminum alloys. *Metall Mater Trans B.* 2006;37(6):887.
- [30] Hansen N. Hall-Petch relation and boundary strengthening. *Scr Mater.* 2004;51(8):801.
- [31] Viala J, Bosselet F, Laurent V, Lepetitcorps Y. Mechanism and kinetics of the chemical interaction between liquid aluminum and silicon-carbide single crystals. *J Mater Sci.* 1993;28(19): 5301.
- [32] Pech-Canul MI. Aluminum alloys for Al/SiC Composites. In: Ahmad Z, editor. *Recent Trends in Processing and Degradation of Aluminum Alloys.* Shanghai: InTech; 2011. 299.
- [33] Lee JC, Byun JY, Park SB, Lee HI. Prediction of Si contents to suppress the formation of Al<sub>4</sub>C<sub>3</sub> in the SiCp/Al composite. *Acta Mater.* 1998;46(5):1771.
- [34] Bao S, Tang K, Kvithyld A, Engh T, Tangstad M. Wetting of pure aluminum on graphite, SiC and Al<sub>2</sub>O<sub>3</sub> in aluminum filtration. *Trans Nonferrous Metals Soc China.* 2012;22(8):1930.
- [35] Yang H, Gu M, Jiang W, Zhang G. Interface microstructure and reaction in Gr/Al metal matrix composites. *J Mater Sci.* 1996;31(7):1903.
- [36] Kobashi M, Choh T. The wettability and the reaction for SiC particle/Al alloy system. *J Mater Sci.* 1993;28(3):684.
- [37] Huber T, Degischer H-P, Lefranc G, Schmitt T. Thermal expansion studies on aluminum-matrix composites with different reinforcement architecture of SiC particles. *Compos Sci Technol.* 2006;66(13):2206.
- [38] Chawla N, Deng X, Schnell D. Thermal expansion anisotropy in extruded SiC particle reinforced 2080 aluminum alloy matrix composites. *Mater Sci Eng A.* 2006;426(1):314.
- [39] Mummery P, Derby B. The influence of microstructure on the fracture behaviour of particulate metal matrix composites. *Mater Sci Eng A.* 1991;135:221.
- [40] Cöcen Ü, Önel K. Ductility and strength of extruded SiCp/aluminum-alloy composites. *Compos Sci Technol.* 2002;62(2):275.

- [41] Arpon R, Molina J, Saravanan R, Garcia-Cordovilla C, Louis E, Narciso J. Thermal expansion behaviour of aluminum/SiC composites with bimodal particle distributions. *Acta Mater.* 2003;51(11):3145.
- [42] Lewandowski J, Liu C, Hunt W Jr. Effects of matrix microstructure and particle distribution on fracture of an aluminum metal matrix composite. *Mater Sci Eng A.* 1989; 107:241.
- [43] Wang Z, Song M, Sun C, He Y. Effects of particle size and distribution on the mechanical properties of SiC reinforced Al–Cu alloy composites. *Mater Sci Eng A.* 2011;528(3):1131.